Role of microbial mats and high sedimentation rates in the early burial and preservation of footprints in a siliciclastic tidal flat

Diana G. Cuadrado [a,b*], **Lucía Maisano** [a,b], **I. Emma Quijada**[c]

[a] Instituto Argentino de Oceanografía (IADO-CONICET-UNS), Florida 5000, 8000 Bahía Blanca, Buenos Aires, Argentina.

[b] Departamento de Geología, Universidad Nacional del Sur, Av. Alem 1253, Cuerpo B´ Piso 2º, 8000 Bahía Blanca, Buenos Aires, Argentina

[c] Departamento de Geología, Universidad de Oviedo, C/ Jesús Arias de Velasco s/n, 33005 Oviedo, Spain

Email: [redacted]@criba.edu.ar; [redacted]@iado-conicet.gob.ar; [redacted]@uniovi.es

* Corresponding author at: Instituto Argentino de Oceanografía (IADO-CONICET-UNS), Florida 5000, 8000 Bahía Blanca, Buenos Aires, Argentina. E-mail address: [redacted]@criba.edu.ar (Diana G. Cuadrado)

ABSTRACT

Sedimentary processes in a microbial flat, developed in a progradational environment and trampled by vertebrates, were monitored under varying energetic conditions. A vertebrate footprint made on the sedimentary surface was selected and was kept under observation along two years visited on nine field trips. Thus, this contribution provides a detailed analysis of the evolution of a microbial tidal flat with high sediment flux events contributing to the better understanding of the sedimentary processes involved in the preservation of a true track. The study demonstrates that the formation of biolaminites (sequence of microbial mats interbedded with sand layers) in the coastal environment is caused by episodic pulses in the hydrodynamic regime of the area. By means of a detailed inspection of a cross-section of a sedimentary block containing the vertebrate footprint, the sedimentation history since the footprint creation is unravelled in relation to the hydrodynamic records. The water energy was inferred using the measurements of a water-level sensor located on the tidal flat recording continuously every 10 minutes. The results indicate that the seawater enters into the zone by floods that occur during storm surges, reaching up to 70 cm height in column water, and transporting abundant sediment, which produce the deposition of flat sand layers or sand ripples on the microbial mats. A sedimentation rate of 0.32 to 0.41 cm per year was calculated along the two-years monitoring. The study recognizes the plastic behaviour of the microbial mat, one of their most important rheological properties, as a response to the registration of a vertebrate footprint. Petrographic analysis of microbial mat layers reveals the precipitation of thin carbonate laminae during periods of seawater evaporation, which may enhance the preservation of the sediments. The episodic sediment transport, in addition to the microbial mat presence, creates the perfect conditions for registration, early burial and preservation of the footprint in siliciclastic sediments.

Keywords: Biostabilization; Biofilm; Track; Ichnology; Plastic deformation; Patagonia (Argentina).

INTRODUCTION

The study of trackways in sedimentary rocks contributes not only to taphonomic interpretation, but also to palaeoenvironmental studies. As demonstrated by Genise et al. (2009), the type, formation, and preservation of fossil footprints is significantly influenced by the environment and sediment features. Consequently, vertebrate tracks may be useful to infer the palaeoenvironment as they provide clues to interpret the substrate conditions at the time of registration (Currie et al. 1991; Marty et al. 2009) and also the post-registration processes defined by Marchetti et al. (2019) as track biostratinomy.

One of the environmental factors that contribute to the good preservation of footprints is flooding, which provides wet fine-grained sediment for epichnal impression, followed by periodic high sedimentation rates, which insure a quick burial of tracks (Scrivner and Bottjer 1986). Lockley and Conrad (1989) stated that footprint preservation is possible due to the presence of a clay drape and a difference between the substrate and the infilling sediment. Seilacher (2008) provided a similar interpretation for the preservation of arthropod trackways, stating that the presence of a clay drape or a film separating the substrate and the casting material is necessary to preserve the track because it prevents amalgamation of both layers. There is also a great agreement on the fact that fine-grained sediments favour a good preservation. Tucker and Burchette (1977) established that the presence of mud (≈ 20%) make the sediment much more cohesive to mould, and Scrivner and Bottjer (1986) agreed on a direct relation between the increase in mud content and the preservation potential of tracks. In this sense, many fossil tracks are found in fine sandstone interlaminated with siltstone-mudstone sediment deposited in sedimentary environments at or near the paleo-watertable all over the world: in mudflat and shallow lacustrine deposits (Upper Cretaceous Jindong Formation, Korea, Paik et al. 2001), in tidal flat and channel to swamp deposits (Lower Cretaceous Dakota Formation, USA, Phillips et al. 2007; Noffke et al. 2019), in tidal flat deposits (Lower Cretaceous Agrio Formation, Argentina, Fernández and Pazos 2013; Lower Cretaceous Oncala Group, Spain, Quijada et al. 2016; Upper Jurassic Villar del Arzobispo Formation, Spain; Campos-Soto et al. 2017), or in floodplain deposits (middle Permian Abrahamskraal Formation, South Africa, Cisneros et al. 2020).

The content of water in sediments is crucial in track penetration depth (Currie et al. 1991). In addition, the rheological properties are also important, such as the plastic behaviour that cohesive sediments have, being essential to produce footprint deformation (Currie et al. 1991; Paik et al. 2001; Phillips et al. 2007). In that sense, microbial mats colonizing the sediment contribute to create the adequate rheological behaviour for deformation of the sediment laminae, besides their great role in preservation (Conti et al. 2005; Marty et al. 2009). Microbial mats elucidate also why undertracks are formed in laminated sediments, composed of alternating sandstone and siltstone-mudstone (Paik et al. 2001; Aramayo et al. 2015; Mujal and Schoch 2020). In this regard, the role of microbial mats in the registration and preservation of vertebrate traces and tracks is recognized as a main factor (Dai et al. 2015).

This study was carried out in a progradational coastal environment that experiences several pulses of seawater inundations and consequent sediment transport. By means of the monitoring of a footprint along two years under different hydrodynamic conditions, the objective of this contribution is twofold. The first objective is to provide a detailed analysis of the evolution of a tidal flat, colonized by microbial mats. The long-term monitoring allowed us to analyse the characteristics of the sedimentary processes that took place after the creation of the footprint, involving the complete burial of a track and a sand ripple formation at the top of the sedimentary surface. The second objective is to contribute to the better knowledge of sedimentary processes involving the preservation of a true track. Otherwise, the results of this study provide insights into coastal processes in a progradational environment and contribute to understand and recognize the role of microorganisms forming microbial mats in a sedimentary sequence.

Study area

The study was carried out in Paso Seco, in northern Patagonia (40° 38.11´S; 62°12.5´W; Fig. 1A), which is a narrow coastal flat formed as the result of the creation of a littoral sand spit 1.6 km wide in its mouth (Cuadrado et al. 2015). The studied coastal flat has been exposed for 100 years ago (Espinosa and Isla 2011), and at the present time, is frequently inundated, especially in winter, when the local sea level rises above the sand spit during storm surges, caused by a low-pressure centre in the Atlantic Ocean moving in a SW to NE direction (Stempels Bautista 2019) (Fig. 1B). The storm surge causes the seawater to breach the sand spit and produces a longitudinal flood current over Paso Seco flat, which may be fast enough to tear the microbial mats present in the flat and produce erosional pockets, mat folds and mat roll-ups (Maisano et al. 2019). A direct relationship between the energy of the current and the height of the water column above the flat has been observed during the sudden flooding produced by storms (Maisano et al. 2019). As a result, depending on the energy of the storm, the zone is flooded between 10 and 70 cm of water column. Subsequently, ebb currents flow slowly and seawater is retained due to a topographic gradient dipping gently landwards, which produces a semi-closed basin colonized by an impermeable microbial mat (Perillo et al. 2019). When seawater is retained in the flat, it progressively evaporates and salinity increases, triggering the precipitation of well-defined and laterally-continuous carbonate laminae (Maisano et al. 2020). There are no fluvial inputs as no rivers are present in the area. Furthermore, animals can travel through the flat, when the flat is subaerially exposed or when it is covered by cm-deep seawater (Fig. 1C, D).

The alternation between quiescence and flooding events provides optimal conditions to form epibenthic microbial mats, covering an area of ca 1.8 km^2 in size. The thick microbial mats (≈ 1 cm) form a coherent carpet-like network of mucilagenous filaments mainly of cyanobacteria, fixed by high amount of EPS (extracellular polymeric substances) (Cuadrado and Pan 2018). The epibenthic microbial mat is present in a supratidal zone that is exposed during several days to weeks between inundations. Epibenthic mats are resistant organic layers on top of the sediment that stabilize the substrate by a magnitude of up to 12 relative to uncolonized sediments (Noffke 2010). In contrast, endobenthic microbial mats typically formed in the intertidal zone (flooded once or twice a day) stabilize the sediments by a magnitude of 3 to 5.

Several vertebrates as *Rhea pennata* and wild pigs, among others, are common habitants in the area of study. Several trackways are found crossing the microbial mats. The abundance of trackways suggest that the vertebrates use the zone as a path when seeking food and water in the surroundings (Fig. 1C, D), and thus, show that these continental vertebrates can visit coastal environments characterized by marine processes.

METHODOLOGY

This study analyses the modifications produced by footprints of *Rhea pennata* in the sediment of Paso Seco and their sediment infill. For this purpose, the sediment compression of two different footprints was compared. On one hand, the first footprint was analysed immediately after it was registered by cutting a cross section through it, which allowed the observation of the mechanical modification produced by the vertebrae in the subjacent sedimentary horizons.

On the other hand, the second footprint was subject to a two year-long monitoring before its removal and cross cutting. In November 2016, a vertebrate footprint left by *Rhea pennata* was selected on the flat to study its evolution through time. The location of the footprint was marked with a coloured steel frame (10 × 10 cm) that included the whole sole. The surface expression of the footprint was monitored by visiting the site in nine occasions during the following two years to observe and photograph the modifications through time. A sedimentary block containing the footprint was recovered in December 2018. The sedimentary block containing the footprint was taken to the laboratory to cut it in cross section to observe the sediment fill. In order to analyse the sediments deformed by the footprint and the infilling in detail, two thin sections were prepared for petrographic analysis from samples taken from the sedimentary block containing the footprint. Thin sections were petrographically analysed in a Nikon Eclipse POL 50i transmitted-light microscope, coupled with a camera.

The inundations of the flat were recorded by a water level logger (HOBO by Onset-model U20; 2.5 cm diameter and 15 cm length; Onset Computer Corporation, Bourne, MA, USA) continuously along two entire years from 2016 to the end of 2018, with an only interruption during Austral summer from November 2017 to February 2018. The sensor was deployed in a vertically buried, perforated PVC pipe, 40 cm in length. The water- and air-pressure, and water temperature parameters were measured every 10 minutes, and the data were corrected by another sensor data located in a higher level, which measured only atmospheric pressure. The water level is referred to the tidal flat.

RESULTS

Development of biolaminites

The flat in Paso Seco is composed of biolaminites (vertical sequences of mat laminae and sandy layers; Fig. 2A). The microbial mats are organic layers constructed by the activity of microbial communities (largely filamentous cyanobacteria), and are characterized by a conspicuous thin lamination, which can be recognized macroscopically (Fig. 2B).

In November 2016, when the monitoring of the footprint was initiated, the flat was covered by a ≈ 1 mm-thick diatom-rich biofilm like a paper, made up of pennate diatoms, which protected the greenish filamentous cyanobacteria layer underneath (Fig. 2B). Beneath the surficial centimetres (more than 4 cm deep), there were condensed layers of buried mats interbedded with up to 1 cm-thick sand layers (Fig. 2C), which are indicative of episodic strong energy events that occur during storm surges (see Study area section). The buried interbedded mats and sand layers show occasionally an undulating shape, instead of a parallel-laminated appearance, which is probably related with microbial deformation structures produced during high energy events (see Maisano et al. 2019).

Monitoring of the depositional surface through time

The surface of the flat in November 2016 was covered by a dried-biofilm, an organic coat like a paper that showed some collapsed bubbles (Fig. 3A; black arrows in Fig. 3B) and small broken bubbles in the surface of the sole (white arrows in Fig. 3C). Interestingly, the dried biofilm derived from a highly hydrated biofilm that was observed four months before (in July 2016, austral winter), when the flat was entirely covered by seawater (Fig. 3D, E). This thick biofilm was highly impermeable as shown by the fact that air bubbles (produced by photosynthetic activity of surficial microorganisms) were retained inside it (Fig. 3D), and also in a thinner biofilm documented over the sediment (Fig. 3E). Both the surface microbial mat trampled by the vertebrate and the underlying sediment were compressed by the footprint (Fig. 3A, B). The small broken bubbles present in the surface of the tracked sediment (white arrows in Fig. 3C) were produced by photosynthetic activity on the surficial microbial mat after the formation of the track.

Four months later, in March 2017, the flat was inundated by a sheet of seawater moved by the wind, which made the observation of the footprint difficult (Fig. 3F). In May, a thin sheet of calm seawater covered the flat, which allowed the research team to see bubbles produced by photosynthetic activity in the water-sediment interface, and patches of a yellowish-beige diatom-rich biofilm with a circular shape at the sedimentary surface (Fig. 3G-H). Comparison of the initial footprint with the state at that time was possible by using the frame as a reference (shown in Fig. 3A) for overlapping with the photograph taken in May (yellow dashed-lines in Fig. 3G). This enabled observing two digit impressions completely refilled by a biofilm, but their borders were still preserved (Fig. 3G). Four and five months later, in September and October, the footprint was almost completely refilled and the tenuous border of the digits could be identified (Fig. 3I-J).

After the austral summer, in March 2018, the footprint was completely refilled and only a vestige of the deeper incisive front part of the claw mark was observed (Fig. 4A). At that time, the epibenthic microbial mat showed a flat surface, which was abruptly modified ten months later (in December), when the flat was covered by undulated bedforms made during severe storms in the previous austral winter (Fig. 4B; see further explanation in Section 4.5). The flat was widely covered by 2D and some 3D asymmetrical ripples with heights < 1 cm and wavelengths between 8 and 10 cm (Fig. 4C-D). Only the top layer (< 1 cm) formed by sand ripples resting on the epibenthic mat was oxic. Below this layer the sediments were anoxic and displayed planar bedding (Fig. 4E).

Vertical variation of the bedding of the host sediment and sediment infill of the footprint

The mechanical modification produced by the vertebrate is revealed in a vertical section cutting several subjacent sedimentary horizons (Fig. 5). The sediment compression of two different footprints was compared. The first one was analysed immediately after it was made (Fig. 5A). The other one was removed from the area two years later (Fig. 5B). Both tracks presented similar deformation immediately below the track in a vertical profile (Fig. 5C, D). The plastic deformation transferred downward into the underneath layers depended on the force applied by different digits (Fig. 5C), being less pronounced in depth. Consequently, the sand layers interbedded with the microbial mats in depth were also compressed (Fig. 5C). At the edge of the sole, the layered sediments are fissured and a sharp track wall is observed (arrow in Fig. 5D).

The whole vertical section of the footprint extracted two years after its registration is comprised of the following layers, from the bottom to the surface (Fig. 5E): i) a 11 mm-thick microbial mat layer that includes several mat sublayers (microbial colonization) separated by very thin sand sheets, which was severely compressed up to 6 mm under the sole (dashed red lines in Fig. 5E); ii) a 4 mm-thick sand layer that overlies the basal microbial mat (S1 in Fig. 5E); and iii) a 2-4 mm-thick microbial mat, which corresponds to the tracking surface (white dashed-lines in Fig. 5E). There are two fissures at both sides of the sole (probably amplified by the recovery work). Once the footprint was formed, a thin microbial mat covered the true track (yellow line in Fig. 5E), and was subsequently covered by two sand layers, the first one only refilled the footprint depression and the last one was deposited over the whole sediment flat. On top of the continuous sand layer a microbial mat colonized the sedimentary surface. Lastly, a sand ripple was formed over the microbial mat with a height of 0.5 cm and a wavelength of 8.5 mm. A thin biofilm capped the crest of the asymmetrical ripple (orange dashed-line in top of Fig. 5E), before a subsequent sand deposition was documented.

Petrographic analysis

Petrographic analysis shows in detail the deformed sediment layers below the tracked surface (Fig. 6). The trampled surface displays an uneven concave shape, and small broken pieces of microbial mat produced by the mechanical pressure of the vertebrate (discontinuous upper red dashed-line in Fig. 6B, C). The sole was filled during a storm by fine sand, composed mainly of quartz, feldspar, amphibole, pyroxene, volcanic rock fragments, and opaque grains (yellow arrow in Fig. 6B-C). At the left side of the thin section, the deformation produced in the sediments by the stepping of the vertebrate is clearly seen, and affects several 0.5-1 mm-thick microbial mats (mm1, mm2 and mm3 in Fig. 6D, E) separated by fine sand laminae (~2 mm thick), which form the typical lamination.

The detailed inspection of the 2.5 mm-thick microbial mat where the vertebrate stepped (area between red dash lines in Fig. 6B-C) shows different appearance from top to base. At the top, cloudy dark brownish organic matter occurs (om in Fig. 6B, C) and, beneath it, a brownish continuous layer around 1.5 mm in thickness and composed of several laminae is present (mm1 in Fig. 6B, C). A separation between om and mm1 is observed currently, which was probably produced during thin section preparation. The brownish layer of the microbial mat is formed by several organic sheets (up to ~60 μm thick) separating thin layers of fine sediment and organic matter, and contains also dispersed sand grains (Fig. 6F, G). Some of the layers of the microbial mat contain lenses of micritic calcite that may coalesce into up to 100 μm-thick discontinuous laminae, which are clearly identified by the comparison under plane- and cross-polarised light (Fig. 6H, I). This carbonate is surrounded by brownish organic matter sheets (red arrows in Fig. 6H, I).

The last layer of sediment to fill the footprint exhibits a ripple bedform at the surface (see Fig. 6A; red arrow in Fig. 7A) resting on a 1 mm-thick microbial mat (yellow bracket in Fig. 7A). A close-up of this microbial mat reveals that it is composed of brownish organic matter sheets

(~20 μm thick) separating sand layers, fine sediment layers and micritic layers (orange, red and yellow arrows, respectively, in Fig. 7B, C), all of them containing dispersed brownish cloudy organic matter.

A detailed analysis of the uppermost surface reveals that the sand ripple (5.5 mm height) was deposited on top of a sharp planar surface over the microbial mat (Fig. 7A). An organic layer (biofilm) of varying thickness was developed over the ripple. The biofilm is less than 100 μm on the crest of the ripple and ~1 mm thick in the trough. Another sand ripple (1 mm ripple height) was deposited over this biofilm (Fig. 7A, D, E), which is overlain by a ~500 µm-thick continuous carbonate layer, lastly covered by an organic matter lamina (Fig. 7F, G).

Hydrodynamic pattern

The analysis of the seawater level over the microbial flat over two years (Fig. 8) makes possible to infer the energy of the inundations into the area, taking into account that previous studies have demonstrated a direct relationship between water height above the flat during sudden floodings and the velocity of the flood current (Maisano et al. 2019). Water temperature, in contrast, is in close relation with seasonal variations (Fig. 8).

The footprint was created prior to November 2016 (pink arrow in Fig. 8A). Afterwards, in December 2016, there were moderate inundations (> 30 cm over the plain) followed by a subaerial exposure that lasted for more than a month coinciding with high radiation in austral summer (January 2017), when the water temperature reached 29 °C and the water table descended to the minimum level below the flat (> 40 cm deep). From February to May 2017 there were recurrent low inundations (< 30 cm). From May and during the austral winter, a relatively constant water lamina was present over the microbial flat (water temperature about 10 °C). Immediately after the field trip in May 2017, three events of moderate inundation (> 30 cm) occurred. One of them raised the water column up to 50 cm in height (Fig. 8A). During 2018, a severe storm that occurred in June provoked a 70 cm-deep inundation, followed by another moderate inundation (> 30 cm) in July (Fig. 8B). After the flooding in July the water level remained at the sediment surface for almost a month, and subsequently descended, causing subaerial exposure of the flat.

DISCUSSION

Significance of the microbial activity for footprint generation and preservation

The optimum preservation potential of vertebrate impressions occurs in fine-grained laminated sediments, either siliciclastic (Thulborn and Wade 1989; Currie et al. 1991; Scarboro and Tucker 1995; Tucker and Burchette 1977; Paik et al. 2001; Benton et al. 2012; Lockley and Xing 2015) or carbonatic (Avanzini et al. 1997). The characteristic lamination of abundant strata containing vertebrate tracks and the presence of mud drapes in them are typical characteristics of microbial mats growing in tidal flats (Cuadrado 2020), which might suggest that microbial mats were developed in the fossil successions. Actually, abundant publications have established a linkage between the formation and preservation potential of vertebrate impressions and microbial mat presence (e.g. Avanzini 1998; Kvale et al. 2001; Conti et al. 2005; Marty 2005; Noffke et al., 2019). Therefore, the knowledge of the life strategies of microbes in sediments assists in the paleohydraulic and paleoenvironmental interpretation. The characteristic planar lamination in epibenthic microbial mats derives from the horizontal arrangement of cyanobacteria filaments on top of the sedimentary surface, attributed to different growth periods caused after seasonal or episodic events (storms). Older mats are successively overgrown by younger mats due to the migration of the organisms in order to find the most favourable conditions (Stal 2012). The organic arrangement produces a continuous flat lamination. Also, laminated levelling (Noffke et al. 2001) overgrows the trough of ripples, and has been identified in ancient successions in which ripple bedforms and microbial mats occur interbedded (Stimson et al. 2018).

The development of mats is basically controlled by moisture and, therefore, binding and growth of epibenthic microbial mats occur under lasting latencies of more than few weeks (Noffke 2010; Cuadrado 2020). During latency, cyanobacteria can exude large amounts of EPS to resist long periods of drought and large fluctuations of salinity and temperature (Stal 2012). Cuadrado and Pan (2018) reveals that Paso Seco is characterized by the presence of cyanobacteria *Coleofasciculus* (formerly *Microcoleus* according to the revision of Siegesmund et al. 2008), a cosmopolitan species with typical multiple ensheathed filament bundles that create a smooth and uniformly flat topography (Gerdes and Krumbein 1987). The latency in winter provides the microbial mat the necessary conditions to better preserve the morphology of the footprint because wet conditions maintained for long times allow the formation of a surficial biofilm that stabilize the footprint. Afterwards, the sand sediment that buries the footprint is deposited as a consequence of sediment transport during storm events, forming the characteristic biolaminites in the area (microbial mats interbedded with sand sheets; Fig. 2A).

Another important biotic factor to take into consideration as an effect of the microbial mat is the oxic-anoxic geochemical variations in the underlying layers, evidenced by steep microgradients (particularly of oxygen and sulphide; van Gemerden 1993) that cause anoxic black sediments below the surface (≈ 2 mm; Fig. 4E). This underneath layer is colonized by chemoorganotrophic bacteria that decompose the deceased cyanobacteria and EPS, with the help of sulphate as an electron donor (Noffke 2010). Below this layer another chemolithotrophic group is established, decomposing the simple chemical compounds discarded by the chemoorganotrophic bacteria above. This consortium of microbes functions as a cooperative that acts as a complex society (Noffke et al. 2013). The initial energy is provided by sunlight, which is used by the photic surficial layer inhabited by cyanobacteria and pennate diatoms. The photosynthetic activity is revealed by small bubbles in the biofilm or over the sedimentary surface (white arrows in Fig. 3C). The consequence of the geochemical activity by microbial mats in the first mm of the surface is the generation of some authigenic minerals as carbonates, pyrite, or even zeolites if the sediment includes volcanic grains as occurs in Paso Seco, among others that are found in the sedimentary record (Cuadrado et al. 2012), which may enhance the footprint preservation (Scott et al. 2008, 2010; Marty et al. 2009).

Mechanical deformation of microbial mat layers

Many studies document the plastic behaviour of the sediments in which the footprints are preserved, not only in the surficial layer, but also in the underlying horizons (Scrivner and Botjer 1986; Phillips et al. 2007; Marsicano et al. 2010; Lockley and Xing 2015; Heredia et al. 2020). This plastic behaviour may be easily explained in the presence of microbial mats, whose high content in organic matter, especially exopolysaccharides secreted by cyanobacteria (Pan et al. 2019), confer plasticity to the sediment subject to mechanical stress. The rheological properties of microbial mats were measured in a study focused on the response of the mats in Paso Seco to physical disruption by incision and compression pressures (Pan et al. 2019), similar to those that vertebrates might produce on a microbial flat with the claw or the sole of the foot, respectively. That experimental study quantified that the microbial mats were able to withstand a compression of 1.56 to 1.9 kg cm^{-2}, and an incising pressure of 10.5 to 14.5 kg cm^{-2}. In general, a greater force is needed in desiccated mats than in wet mats to deform. This is the reason why footprints are produced more easily under wet conditions, as observed by Marty et al. (2009) in present-day tidal flats. This behaviour could cause that footprints in the microbial mats of Paso Seco are more commonly formed in winter, when the flat is humid or inundated, than in summer, when the flat is dried and footprints would not even be registered. Moreover, in agreement with the experiment results, the mechanical deformation affects differentially the uppermost surface (≈ 5 mm) where the density of living cyanobacteria filaments is highest and capable of withstanding plastic deformation, up to a threshold limit above which the mat fractures (see Fig. 5C, D). This threshold limit was achieved at lower force when the microbial mat was subject to incision pressure, comparable to that exerted by claws, than to compression pressure, comparable to that of the sole of the foot.

The experimental results of Pan et al. (2019) are useful to understand the deformation of the microbial mats and interlayered sands observed in the studied sedimentary blocks. The compressed sediments show a plastic deformation, which affects every layer and occurs at every depth, and locally a mechanical disruption, which breaks the areas subject to higher pressures, such as the footprint edges, and closer to the surface (Fig. 5C-E). Therefore, the pressure applied by the vertebrate produced a general plastic deformation in the compressed sediments and, in the areas that exceeded the plastic threshold limit, the microbial mats and interbedded sand layers were broken. Furthermore, brittle deformation was achieved more easily under the claws than under the sole of the foot, where ductile deformation predominated (Fig. 5A, C), which is consistent with the experimental results that showed that the plastic threshold limit was reached at lower force under incision pressure than under compression pressure (Pan et al. 2019).

Sedimentary evolution of the sequence containing the footprint

In spite that the sea is nearly 4 km far away from the study area, coastal marine processes (i.e. current sediment transport, sand ripple formation) are very relevant in sedimentation in Paso Seco. The analysis of the data obtained by monitoring of the depositional surface and hydrodynamic changes through time, combined with the observations of the host sediment bedding and of the infill of the footprint in cross-section and under petrographic microscope, allows us to reconstruct in detail and to date the sedimentary processes involved in the generation and preservation of the footprint.

The sedimentary evolution of the flat prior to the generation of the footprint (selected on November 2016) is recorded in the deformed sediment underneath the track. The sedimentary surface where the vertebrate walked was formed by biolaminites and was covered by a dried biofilm. This biofilm was made previously, during austral winter season (Fig. 3D, E), when the seawater was retained over the surface nearly for two months (Fig. 9A3). Under petrographic analysis, very small pieces of detached microbial mat are seen on the irregular surface of the stepped mat, which were caused by the mechanical disruption of the mat produced by the stepping (Fig. 6B, C). The tracked microbial mat includes carbonate laminae less than 100 μm thickness, (Fig. 6F-I) probably precipitated during the exposure of the flat in the previous warm months (August - November 2016; Fig. 8A, 9A3).

Footprints in coastal areas are generally filled with sediments transported during storms (Carmona et al. 2011). The footprint here monitored was refilled by sand sediment (0.4 cm thickness) probably by two storms events that occurred after its creation (water column between 30 and 46 cm depth; Fig. 9B3). Successive storm events that occurred in 2017 buried the flat and the footprint with sediment (column water between 35 and 47 cm depth; Fig. 9C3). Subsequently, the footprint and the flat were covered by a thick (0.4 cm) planar microbial mat at the beginning of 2018 (Fig. 9D2). In addition to sand, fine-grained sediment and organic matter layers, the microbial mat contains micritic calcite precipitates (Fig. 7B, C).

An asymmetrical sand ripple of 0.3 cm in height was deposited over the sequence as a consequence of the severe storm that occurred in June 2018 (Fig. 9E2, E3). In that occasion the column water reached 70 cm during two days due to a storm surge, creating several large microbial structures, such as roll-ups, fold structures and flipped-over edges (see details in

Maisano et al. 2019). The ripple was exposed only some days before another storm event in July (Fig. 9E3). This period of latency between storms was enough for the microbial filaments to form a new biofilm (see yellow dashed line in Fig. 7A), creating a sinoidal structure (Noffke 2010; Cuadrado, 2020). The thickness of this biofilm depends not only on the period of subaerial exposure (Noffke, 2010), but on the location relative to the ripple, showing a greater thickness on the trough (yellow dashed line in Fig. 7D, E). Probably, this is due to greater moisture for a longer time on the trough than on the crest ripple during periods of non-deposition (Gerdes and Krumbein 1987). A subsequent storm (July 2018, Fig. 9E2, E3) created another ripple (1 mm width) lying over the previous one (orange arrow Fig. 7A). The subsequent latency period, which lasted several months under temperate weather (Fig. 9E), allowed the formation of a new thick biofilm (~500 µm thickness), composed of a continuous carbonate layer under an organic sheet (Fig. 7D-G). Carbonate precipitation in the biofilm was probably related with seawater evaporation that eventually led to subaerial exposure of the flat on windy conditions (Maisano et al. 2020).

All these considerations help to understand how the sedimentary processes that take place in a present-day supratidal flat colonized by microbial mats are recorded in sediments, which may be applicable to interpret fossil successions. The burial of the monitored footprint was caused by energetic floodings during storm surges, followed by periods of latency. In the present study, three strong flooding events were recorded as sand layers and relatively long (several weeks) latencies were recorded as biofilms or microbial mats (Fig. 10).

Early lithification and sedimentation rate as factors contributing to footprint preservation

The calcium carbonate precipitates observed in the biofilms and microbial mats of Paso Seco enhance the preservation potential of the footprints because they cause early lithification of sediments. Early lithification of microbial mats induced by bacterially-induced carbonate precipitation has been described in abundant examples in the literature (e.g. Krumbein and Cohen 1977; Chafetz and Buczynski 1992). In the case of Paso Seco, the interaction between biotic and abiotic factors is crucial to create the conditions for carbonate precipitation (Maisano et al. 2020). The semi-closed saline basin, warm temperatures and strong winds contribute to periodic seawater evaporation in the coastal flat, in which the microbial mat acts as an impermeable layer and contribute to retain a shallow water column covering the flat. The periodic seawater evaporation leads to calcium carbonate supersaturation. Thus, laterally-continuous carbonate laminae are commonly formed in the microbial mats or in the biofilms covering the sand ripples. As a consequence, on one hand, carbonate laminae present in the host sediment, which are subject to plastic deformation during footprint formation as the rest of the mat layers (Fig. 6), may help to identify this type of structures in the sedimentary record. On the other hand, the formation of carbonate laminae in the sediment infill of the footprint contributes to the burial and lithification of the footprint.

Another factor that needs to be taken into consideration when evaluating the preservation potential of the footprint is the sedimentation rate. Measurements of the thicknesses of sediment layers on the analysed sediment block allow calculation of sedimentation rate on the flat. These measurements were performed in the areas outside the depression produced by the footprint and did not include the uppermost ripples, in order to avoid local variabilities and to provide general values valid for the whole flat. Thus, the block reveals sediment thickness accumulation of 0.7 to 0.9 cm between November 2016 and December 2018, giving a rate of sedimentation of 0.32 to 0.41 cm per year (Fig. 5D, E). However, sedimentation rate was not linear through time, but important differences existed depending on the type of sediment accumulating in the flat in each period. While the microbial mat took five months (October 2017 to March 2018) to reach 0.4 cm in width, a similar thickness of sand can be reached during a storm that takes only one or two days. The two-year monitoring of the track shows that neither erosive processes, nor bioturbation disrupted the footprint, but sediment input gradually buried the track. The relatively high sedimentation rates recorded in the flat, characterized by small pulses of sediment input and periods of latency, created the perfect conditions for footprint preservation. These observations in Paso Seco suggest that ancient sedimentary successions bearing abundant well-preserved vertebrate tracks could have been formed in palaeoenvironments subject to similar sedimentary conditions: pulses of high sedimentation input, plus absence of erosive processes and bioturbation.

CONCLUSIONS

The study presents a real-world research case to better understand the registration process and preservation potential of vertebrate trace fossils, and the role that microbial mats play in the early stabilization of sediments that contain surface ichnofossils. The climate and environmental conditions under which a footprint was registered and preserved were recorded, and the sedimentary processes that affect the preservation of the footprint were analysed by a two year-monitoring of a microbial-mat colonized tidal flat. The study demonstrates that the presence of a microbial mat is the key for the registration of footprints because the microbial activity confers plastic behaviour properties to the sediments that allow deformation of the substrate necessary for the formation of these sedimentary structures. After registration of the footprints, the post-sedimentary processes that take place in the sedimentary environment are crucial for their preservation. Episodic flooding filled the footprint and also created sand ripples. After each flooding event a biofilm or a new microbial mat was formed by binding and growing during latencies, which helped to preserve trace morphology. As a result, a sedimentation rate of 0.3-0.4 cm per year was measured, produced by the inputs of intermittent storm surges forming sand layers of different width, and the following recolonization of the depositional surface. The stabilization is improved by early lithification of the mat due to carbonate precipitation caused by the combination of biotic and abiotic processes. Moreover, the lack of erosive processes, due to the rise of the erosional threshold caused by the microbial mat, and the lack of bioturbation are decisive also for footprint preservation. Therefore, the observations in Paso Seco suggest that ancient successions bearing abundant well-preserved vertebrate tracks could have been formed in coastal palaeoenvironments characterized by similar hydrodynamic characteristics –pulses of high sedimentation input followed by periods of latency– and by the development of microbial mats, which create the perfect conditions for registration, early burial and preservation of the footprint.

ACKNOWLEDGEMENTS

We thank E.A.Gómez and L.A.Raniolo for invaluable help during fieldwork. We also thank the staff of the UNS/INGEOSUR Petronomy Laboratory for the skilful preparation of thin sections. This work was supported by Argentinian CONICET (grant number PIP 2013 N°4061) and SECYT-UNS (grant number PGI 24/H138), as well as by the Spanish Department of Science, Innovation and Universities (project PGC2018-094034-B-C21) and the Spanish Department of Education, Culture and Sports (José Castillejo grants CAS16/00124 and CAS17/00270). We also appreciate the kind comments and valuable suggestions of M. Stimson and an anonymous reviewer, as well as those of the Associate Editor M. Gingras.

REFERENCES

Aramayo, S.A., de Bianco, T.M., Bastianelli, N.V., and Melchor, R.N., 2015, Pehuen Co: Updated taxonomic review of a late Pleistocene ichnological site in Argentina: Palaeogeography, Palaeoclimatology and Palaeoecology, v. 439, p. 144-165.

Avanzini, M., 1998, Anatomy of a footprint: bioturbation as a key to understanding dinosaur walking dynamic: Ichnos, v. 6, p. 129-139.

Avanzini, M., Frisis, S., Van Deer Driessche, K., and Keppens, E., 1997, A dinosaur tracksite in an Early Liassic tidal flat in northern Italy: Paleoenvironmental reconstruction from sedimentology and geochemistry: Palaios, v. 12, p. 538-551.

Benton, M.J., Newell, A.J., Price, G.D., and Kurkin, A.A., 2012, Preservation of exceptional vertebrate assemblages in Middle Permian fluviolacustrine mudstones of Kotel'nich, Russia: stratigraphy, sedimentology, and taphonomy: Palaeogeography, Palaeoclimatology and Palaeoecology, v. 319, p. 58-83.

Campos-Soto, S., Cobos, A., Caus, E., Benito, M.I., Fernández-Labrador, L., Suarez-Gonzalez, P., Quijada, I.E., Mas, R., Royo-Torres, R., and Alcalá, L., 2017, Jurassic Coastal Park: A great diversity of palaeoenvironments for the dinosaurs of the Villar del Arzobispo Formation (Teruel, eastern Spain): Palaeogeography, Palaeoclimatology and Palaeoecology, v. 485, p. 154-177.

Carmona, N.B., Bournod, C.A., Ponce, J.J., and Cuadrado, D.G., 2011, The role of microbial mats in the preservation of bird footprints: a case study from the mesotidal Bahia Blanca estuary (Argentina), *in* Microbial Mats in Siliciclastic Depositional Systems Through Time. SEPM (Society for Sedimentary Geology). Special Publication №101.

Chafetz, H. S., and Buczynski, C., 1992, Bacterially induced lithification of microbial mats: Palaios, v. 7, p. 277-293.

Cisneros, J.C., Day, M.O., Groenewald, J., and Rubidge, B.S., 2020, Small footprints expand middle Permian amphibian diversity in the South African Karoo: Palaios, v. 35, p. 1-11.

Conti, M. A., Morsilli, M., Nicosia, U., Sacchi, E., Savino, V., Wagensommer, A., Di Maggio, L., and Gianolla, P., 2005, Jurassic dinosaur footprints from southern Italy: Footprints as indicators of constraints in paleogeographic interpretation: Palaios, v. 20, p. 534-550.

Cuadrado, D.G., 2020, Geobiological model to ripple genesis and preservation in a heterolithic sedimentary sequence in a supratidal area: Sedimentology, v. 67, p. 2747-2763.

Cuadrado, D.G., and Pan J., 2018, Field observations on the evolution of microbial reticulates in a modern siliciclastic coastal environment: Journal of Sedimentary Research, v. 88, p. 24-37.

Cuadrado, D.G., Carmona, N.B., and Bournod, C.N., 2012, Mineral precipitation on modern siliciclastic tidal flats colonized by microbial mats: Sedimentary Geology, v. 271-272, p. 58-66.

Cuadrado, D.G., Pan J., Gómez, E.A., and Maisano, L., 2015, Deformed microbial mat structures in a semiarid temperate coastal setting: Sedimentary Geology, v. 325, p. 106-118.

Currie, P.J., Nadon, G.C., and Lockley, M.G., 1991, Dinosaur footprints with skin impressions from the Cretaceous of Alberta and Colorado: Canadian Journal of Earth Science, v. 28, p. 102-115.

Dai, H., Xing, L.D., Marty, D., Zhang, J., Persons IV, W.S., Hu, H., and Wang, F., 2015, Microbially-induced sedimentary wrinkle structures and possible impact of microbial mats for the enhanced preservation of dinosaur tracks from the Lower Cretaceous Jiaguan Formation near Qijiang (Chongqing, China): Cretacic Research, v. 53, p. 98-109.

Espinosa, M., and Isla, F., 2011, Diatom and sedimentary record during themid-Holocene evolution of the San Blas estuarine complex, northern Patagonia, Argentina: Ameghiniana, v. 48, p. 411–423.

Fernández, D.E., and Pazos, P.J., 2013, Xiphosurid trackways in a Lower Cretaceous tidal flat in Patagonia: Palaeoecological implications and the involvement of microbial mats in trace-fossil preservation: Palaeogeography, Palaeoclimatology and Palaeoecology, v. 375, p. 16-29.

Genise, J.F., Melchor, R.N., Archangelsky, M., Bala, L.O., Straneck, and R. de Valais, S., 2009, Application of neoichnological studies to behavioural and taphonomic interpretation of fossil bird-like tracks from lacustrine settings: The Late Triassic–Early Jurassic? Santo

Domingo Formation, Argentina: Palaeogeography, Palaeoclimatology and Palaeoecology, v. 272, p. 143-161.

Gerdes, G., and Krumbein, W.E., 1987, Biolaminated deposits, *in* Bhattacharya, S. Friedman, G.M. Neugebauer, H.J. Seilacher, A., eds., Lecture Notes in Earth Sciences 9, Springer, Berlin, p. 1-183.

Heredia, A.M., Díaz-Martínez, I., Pazos, P.J., Comerio, M., and Fernández, D.E., 2020, Gregarious behaviour among non-avian theropods inferred from trackways: A case study from the Cretaceous (Cenomanian) Candeleros Formation of Patagonia, Argentina: Palaeogeography, Palaeoclimatology and Palaeoecology, v. 538, p. 109480.

Krumbein, W.E., and Cohen, Y., 1977, Primary production, mat formation, and lithification: Contribution of oxygenic and facultative anoxygenic cyanobacteria, *in* Flügel, E., eds., Fossil Algae, New York, Springer-Verlag, p. 37-56.

Kvale, E. P., Johnson, G. D., Mickelson, D. L., Keller, K., Furer, L. C., and Archer, L. W., 2001, Middle Jurassic (Bajocian and Bathonian) dinosaur megatracksites, Bighorn Basin, Wyoming: Palaios, v. 16, p. 233–254.

Lockley, M., and Conrad, K., 1989, The palaeoenvironmental context, preservation and palaeoecological significance of dinosaur tracksites in western USA, *in* Gillette, D. D. Lockley, M. G., eds, Dinosaur tracks and traces. Cambridge University Press, Cambridge, p. 121–134.

Lockley, M.G., and Xing, L., 2015, Flattened fossil footprints: implications for paleobiology: Palaeogeography, Palaeoclimatology and Palaeoecology, v. 426, p. 85-94.

Maisano, L., Cuadrado, D.G., and Gómez, E.A., 2019, Processes of MISS-formation in a modern siliciclastic tidal flat, Patagonia (Argentina): Sedimentary Geology, v. 381, p. 1-12.

Maisano, L., Quijada, I.E., Cuadrado, D.G., Perillo, V.L., Pan, J., and Martinez A.M., 2020, Carbonate laminae recorded in a siliciclastic tidal flat colonized by microbial mats: Sedimentary Geology, v. 405, p. 105702.

Marchetti, L., Belvedere, M., Voigt, S., Klein, H., Castanera, D., Díaz-Martínez, I., and Farlow, J.O., 2019, Defining the morphological quality of fossil footprints. Problems and principles of preservation in tetrapod ichnology with examples from the Palaeozoic to the present: Earth-Science Reviews, v. 193, p. 109-145.

Marsicano, C.A., Mancuso, A.C., Palma, R.M., and Krapovickas, V., 2010, Tetrapod tracks in a marginal lacustrine setting (Middle Triassic, Argentina): Taphonomy and significance: Palaeogeography, Palaeoclimatology and Palaeoecology, v. 291, p. 388-399.

Marty, D., 2005, Sedimentology and taphonomy of dinosaur track-bearing Plattenkalke (Kimmeridgian, Canton Jura, Switzerland): Zitteliana, B26, p. 20.

Marty, D., Strasser, A., and Meyer, C.A., 2009, Formation and Taphonomy of Human Footprints in Microbial Mats of Present-Day Tidal-flat Environments: Implications for the Study of Fossil Footprints: Ichnos, v. 16, p. 127-142.

Mujal, E., and Schoch, R. R., 2020, Middle Triassic (Ladinian) amphibian tracks from the Lower Keuper succession of southern Germany: Implications for temnospondyl locomotion and track preservation: Palaeogeography, Palaeoclimatology and Palaeoecology, v. 543, p. 109625.

Noffke, N., 2010, Microbial Mats in Sandy Deposits. Elsevier, Amsterdam, p. 196.

Noffke, N., Gerdes, G., Klenke, T., and Krumbein, W.E., 2001, Microbially induced sedimentary structures: A new category within the classification of primary sedimentary structures: Journal of Sedimentary Research, v. 71, p. 649-656.

Noffke, N., Decho, A.W., and Stoodley, P., 2013, Slime through time: the fossil record of prokaryote evolution: Palaios, v. 28, p. 1-5.

Noffke, N., Hagadorn, J., and Bartlett, S., 2019, Microbial structures and dinosaur trackways from a cretaceous coastal environment (Dakota Group, Colorado, U.S.A.): Journal of Sedimentary Research, v. 89, p. 1096-1108.

Paik, I.S., Kim, H.J., and Lee, Y.I., 2001, Dinosaur track-bearing deposits in the Cretaceous Jindong Formation, Korea: occurrence, palaeoenvironments and preservation: Cretaceous Research, v. 22, p. 79-92.

Pan, J., Perillo, V.L., and Cuadrado, D.G., 2019, Quantification of microbial mat response to physical disruption in siliciclastic sediments: Estuarine, Coastal and Shelf Science, v. 230, p. 106434.

Perillo, V.L., Maisano, L., Martinez A.M., Quijada I.E., and Cuadrado D.G., 2019, Microbial mat contribution to the formation of an evaporitic environment in a temperate-latitude ecosystem: Journal of Hydrology, v. 575, p. 105–114.

Phillips Jr, P.L., Ludvigson, G.A., Joeckel, R.M., González, L.A., Brenner, R.L., and Witzke, B.J., 2007, Sequence stratigraphic controls on synsedimentary cementation and preservation of dinosaur tracks: example from the lower Cretaceous (Upper Albian) Dakota Formation, Southeastern Nebraska, USA: Palaeogeography, Palaeoclimatology and Palaeoecology, v. 246, p. 367-389.

Quijada, I.E., Suarez-Gonzalez, P., Benito, M.I., and Mas, R., 2016, Tidal *versus* continental Sandy-muddy flat deposits: Evidence from the Oncala Group (Early Cretaceous, N Spain), *in* Tessier, B., and Reynaud, J.-Y., eds., Contributions to Modern and Ancient Tidal Sedimentology: IAS, Special Publication 47, p. 133-159.

Scarboro, D.D., and Tucker, M.E., 1995, Amphibian footprints from the mid-Carboniferous of Northumberland, England: Sedimentological context, preservation and significance: Palaeogeography, Palaeoclimatology and Palaeoecology, v. 113, p. 335-349.

Scott, J.J., Renaut, R.W., and Owen, R.B., 2008, Preservation and paleoenvironmental significance of a footprinted surface on the Sandai Plain, Lake Bogoria, Kenya Rift Valley: Ichnos, v. 15, p. 208-231.

Scott, J.J., Renaut, R.W., and Owen, R.B., 2010, Taphonomic controls on animal tracks at saline, alkaline Lake Bogoria, Kenya Rift Valley: impact of salt efflorescence and clay mineralogy: Journal of Sedimentary Research, v. 80, p. 639-665.

Scrivner, P.J., and Bottjer, D.J., 1986, Neogene avian and mammalian tracks from Death Valley National Monument, California: their context, classification and preservation: Palaeogeography, Palaeoclimatology and Palaeoecology, v. 57, p. 285-331.

Seilacher, A., 2008, Biomats, biofilms, and bioglue as preservational agents for arthropod trackways. Palaeogeography, Palaeoclimatology and Palaeoecology, v. 270, p. 252-257.

Siegesmund, M.A., Johansen, J.R., Karsten, U., and Friedl, T., 2008, Coleofasciculus gen. nov. (Cyanobacteria): Morphological and Molecular Criteria for Revision of the Genus microcoleus gomont 1: Journal of Phycology, v. 44, p. 1572-1585.

Stal, L.J., 2012. Cyanobacterial mats and stromatolites, *in* Whitton B., eds., Ecology of Cyanobacteria II. Springer, Dordrecht, p. 65-125.

Stempels Bautista, C., 2019, Ondas de tormenta en la zona costera de Paso Seco, Buenos Aires, Argentina [B Thesis]: Universidad Nacional del Sur, Argentina, 60 pp.

Stimson, M., Macrae, A., Miller, R.F., Hinds, S.J., Minter, N.J., Prescott, Z., Redden, B., Macneil, M., Cron, S., and Foster, S.A.M., 2018, *Rugalichnus mclaughlinensis*: a new ichnospecies of microbially induced sedimentary structure from the nonmarine Early Carboniferous of New Brunswick, Canada, in Lucas, S.G., and Sullivan, R.M., eds., Fossil record 6: New Mexico Museum of Natural History and Science, Bulletin 79, p. 673-689.

Thulborn, R.A., and Wade, M., 1989, A footprint as a history of movement. Dinosaur tracks and traces. Cambridge University Press, Cambridge, p. 51–56.

Tucker, M.E., and Burchette, T.P. 1977, Triassic dinosaur footprints from South Wales: their context and preservation: Palaeogeography, Palaeoclimatology and Palaeoecology, v. 22, p. 195-208.

Van Gemerden, H., 1993, Microbial mats: a join venture: Marine Geology, v. 113, p. 3-25.

Figure captions

Fig. 1. A) Location of the coastal flat of Paso Seco in South America (Argentina in blue). The study area, marked by an orange dashed-line, is limited by the cul-de-sac of a tidal channel and a sand spit. The yellow arrow indicates the view of (B). B) Oblique view of the study area showing the width of the microbial mat area and the sand spit. C) Schematic diagram of (B) showing the relative height of the relief above sea level. D) Vertebrate tracks observed on the tidal flat when it is subaerially exposed.

Fig. 2. Characteristic sedimentary core of Paso Seco composed of biolaminite. A) Dark laminae are sand sediment layers and light laminae are organic and fine sediment layers. The top mat is covered by a diatom-rich biofilm. cy: cyanobacteria layer formed by bundled sheaths of *Coleofasciculus*. B) A close-up view of (A) showing a ≈ 1 mm-thick biofilm like a paper, made up of pennate diatoms, which protect the greenish filamentous cyanobacteria layer underneath. C) Buried laminated mats interbedded with sand layers.

Fig. 3. Appearance of the footprint surface between November 2016 and October 2017. A) Flat surface in November 2016 showing the monitored vertebrate footprint. B) A close-up of (A). Collapsed and deformed bubbles are pointed by black arrows. C) A close-up of (B) showing small broken bubbles (white arrows) on the sole. D) Thick biofilm formed in July 2016 (austral winter). E) Thin biofilm (bubbles were retained inside) covering the flat in July 2016. F) Footprint inundated by seawater in March 2017. G) Flat surface covered with a thin sheet of seawater in May 2017. The two digits are delineated by a yellow dash-line. Bubbles produced by photosynthetic activity were developed in the water-sediment interface and circular patches of a yellowish-beige biofilm at the sedimentary surface. H) Close-up view of (G). I) Flat appearance in September 2017. J) Flat surface in October 2017. The footprint is almost levelled.

Fig. 4. Flat surface appearance between March and December 2018. A) The surface in March 2018. Yellow dashed-lines indicate the footprint location. B) Flat surface appearance in December 2018. The flat is covered by asymmetrical current ripples. The direction of flood is pointed by an arrow. C) 2D and 3D asymmetrical ripples exhibited over the footprint in December 2018. D) A close-up of (C) showing an asymmetrical rippled area. E) Vertical section of asymmetrical sand ripples (oxic layer) overlying the epibenthic mat (anoxic layer) that displays planar bedding (yellow dashed lines).

Fig. 5. Plan views and cross sections of the *Rhea pennata* footprints. A) Appearance of the footprint that was extracted immediately after its registration. The transect shows the location where the cut AB was performed. B) Close-view of the monitored footprint on the tidal flat showing the transect where the cut CD was performed after two years. C) Vertical section of (A). MM: microbial mat, S: sand layer. D) Vertical section of (B). The arrow indicates the fissure in the track wall. E) Line drawing of (D) indicating the sediments underneath and over the footprint. The layers underneath the footprint are composed, from the bottom to the surface, of: microbial mat layers separated by thin sand sheets (red dashed lines), sand layer S1, sand sheets between microbial mats (white dashed-lines), and the tracking surface (yellow line). The layers overlying the footprint are composed of: a sand layer and a thin microbial mat levelling the footprint (orange dashed-line), a continuous sand layer covered by a thick microbial mat (limited by white lines), and an asymmetrical ripple with a biofilm at the top (orange dashed-line) capping the sedimentary succession. Two fissures at both sides of the finger compression (white lines) can be observed.

Fig. 6. Petrographic photomicrographs. A) Vertical sedimentary profile of the block containing the monitored footprint showing the location of the thin sections analysed. B) Thin section plane-polarised light photomicrograph showing the sediment deformation after the

vertebrate footprint. The microbial mat where the vertebrate stepped is marked by red dashed lines. Red arrows indicate small broken pieces of the stepped microbial mat. Yellow arrow indicates fine sand. om: organic matter; mm1: microbial mat layer. C) Cross-polarised light photomicrograph of (B). D) Close-up of the microbial mat deformation (yellow square in B) under plane-polarised light. Red dashed-line shows the base of the microbial mat where the vertebrate stepped on (mm1). Yellow dashed-lines delimit microbial mats (mm2 and mm3) separated by fine sand laminae (orange lines). E) Cross-polarised light photomicrograph of (D). F) Close-up of the microbial mat where the vertebrate stepped on (yellow square in B) under plane-polarised light. Micritic carbonate laminae are shown, see location on (G). Red dashed line indicates the base of the microbial mat. G) Schematic diagram of (F). H) Close-up of the laminae in the microbial mat (red square in F) under plane-polarised light. Red arrows show brownish organic sheets and yellow arrows show lenses of micritic calcite. I) Cross-polarised light photomicrograph of (H).

Fig. 7. Petrographic photomicrographs of the surficial part of the sedimentary sequence. A) Thin section cross-polarised light photomicrograph of the sediment overlying the footprint. The yellow bracket indicates a microbial mat; the red arrow indicates a sand ripple; the yellow dashed lines indicate an organic layer (biofilm) of varying thickness; the orange arrow indicates a subsequent sand ripple. B) Plane-polarised light photomicrograph of a close-up of a 1 mm-thick microbial mat (yellow square in A). C) Cross-polarised light photomicrograph of (B). The microbial mat is composed of brownish organic matter sheets (yellow dashed lines), sand layers (orange arrows), micritic layers (yellow arrows), and fine sediment layers (red arrow). D) Close-up of the sand ripples under plane-polarised light (red square in A). Red dashed line indicates the top of the microbial mat over which the ripple lies. Yellow dashed-line indicates the organic layer (biofilm) of varying thickness that covers the ripple. Orange arrow indicates another sand ripple over the biofilm. Green arrow indicates a carbonate lamina covered by an organic matter lamina. E) Close-up of the

trough of the sand ripple under plane-polarised light (red square in A). The yellow dashed line indicates a 1 mm-thick biofilm over the trough. Orange arrow indicates another sand ripple over the biofilm and the green arrow, a carbonate lamina covered by an organic matter lamina. F) Close-up of the biofilm covering the sand ripple under plane-polarised light (yellow square in D). The red arrow shows a carbonate lamina, and the green arrow, an organic matter lamina. G) Cross-polarised light photomicrograph of (F).

Fig. 8. Hydrodynamic regime over the tidal flat. A) Water level and water temperature record from June 2016 to October 2017. Pink arrow shows the beginning of the footprint monitoring. B) Water level and water temperature record from March to December 2018. Pink dashed-lines indicate when the footprint was photographed.

Fig. 9. Evolution of the sedimentary infilling of the footprint along two years. The arrow in A1 indicates the cross section showed in A2. Each step links the surface appearance of the flat with the water level records of the period analysed. A) November 2016. B) May 2017. C) October 2017. D) March 2018. E) December 2018. n/d: no data.

Fig. 10. Relation between cross section of the monitored footprint and hydrodynamic events. A) Footprint cross-section in which the location of the close-up view shown in (B) is indicated. Colour lines are the same as in Fig. 5. B) Close-up view of the sediment cross section with the hydrodynamic log from November 2016 to December 2018. The height of the column water over the tidal flat is a proxy for the hydraulic energy on the flat.

Figure 1

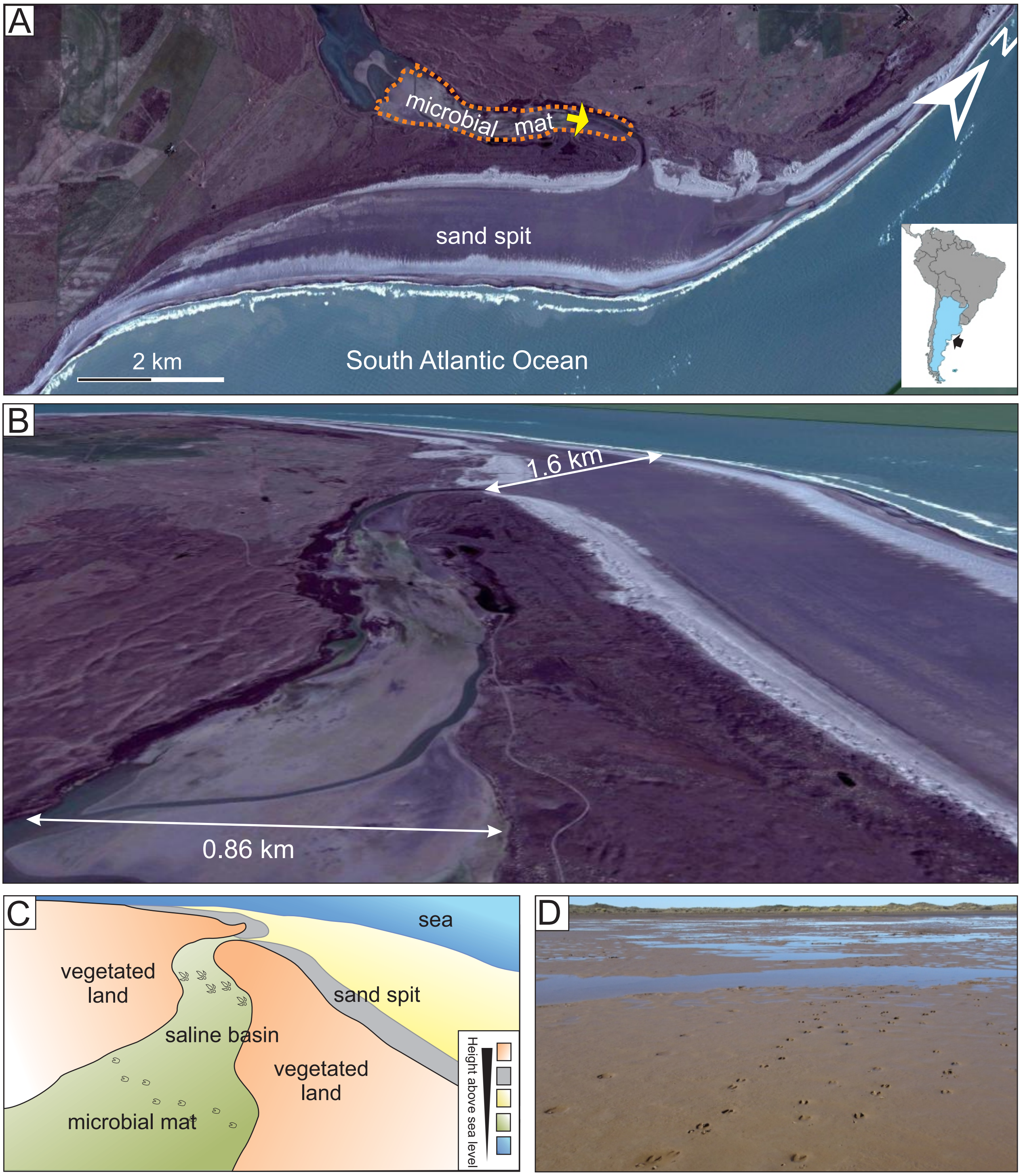
A
microbial mat
sand spit
2 km
South Atlantic Ocean
N
B
1.6 km
0.86 km
C
vegetated land
sea
sand spit
saline basin
vegetated land
microbial mat
Height above sea level
D

Figure 2

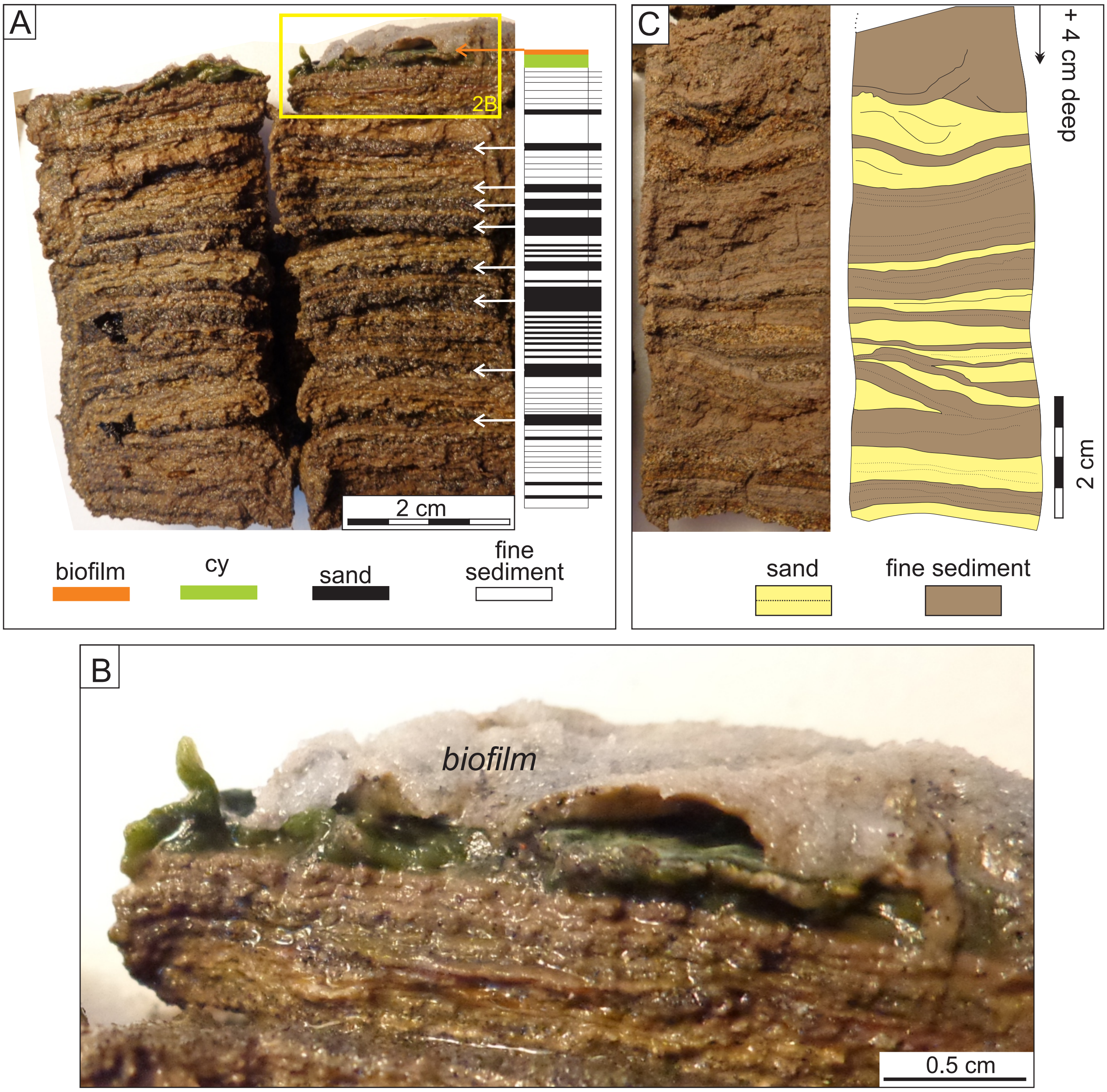
A
2B
2 cm
biofilm
cy
sand
fine sediment
C
+ 4 cm deep
2 cm
sand
fine sediment
B
biofilm
0.5 cm

Figure 3

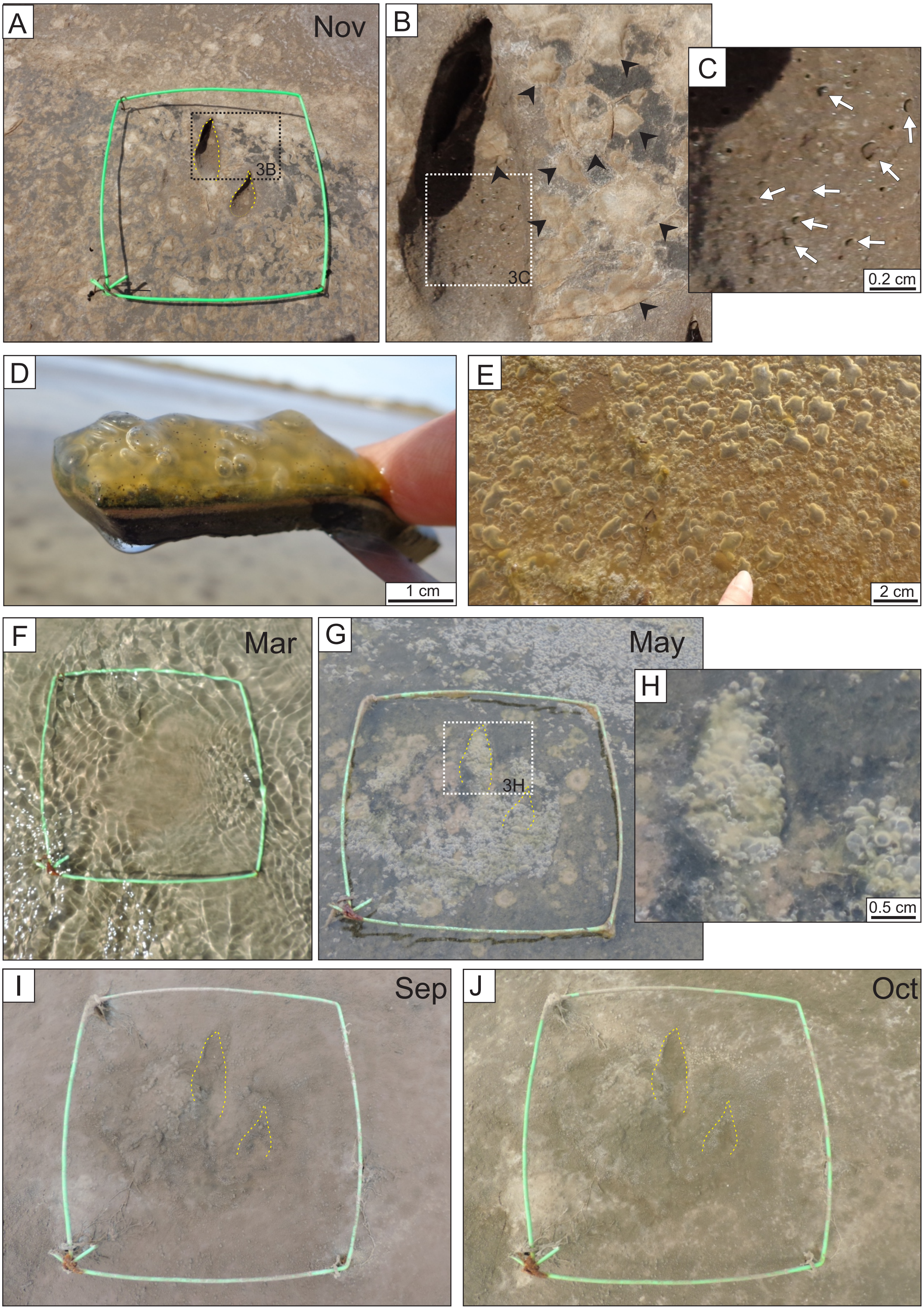

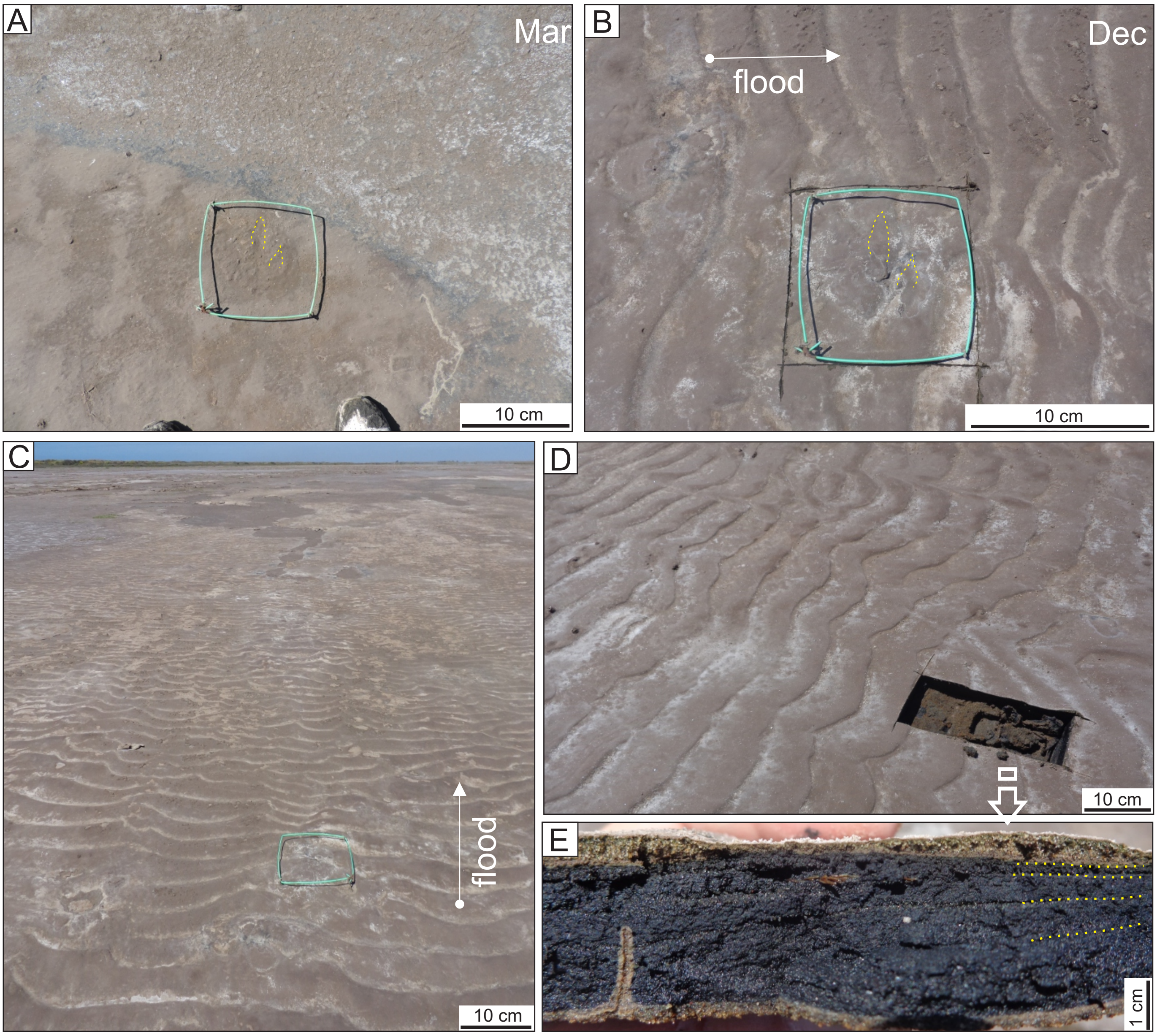
A
Mar
10 cm
B
Dec
flood
10 cm
C
flood
10 cm
D
10 cm
E
1 cm

Figure 5

Figure 6

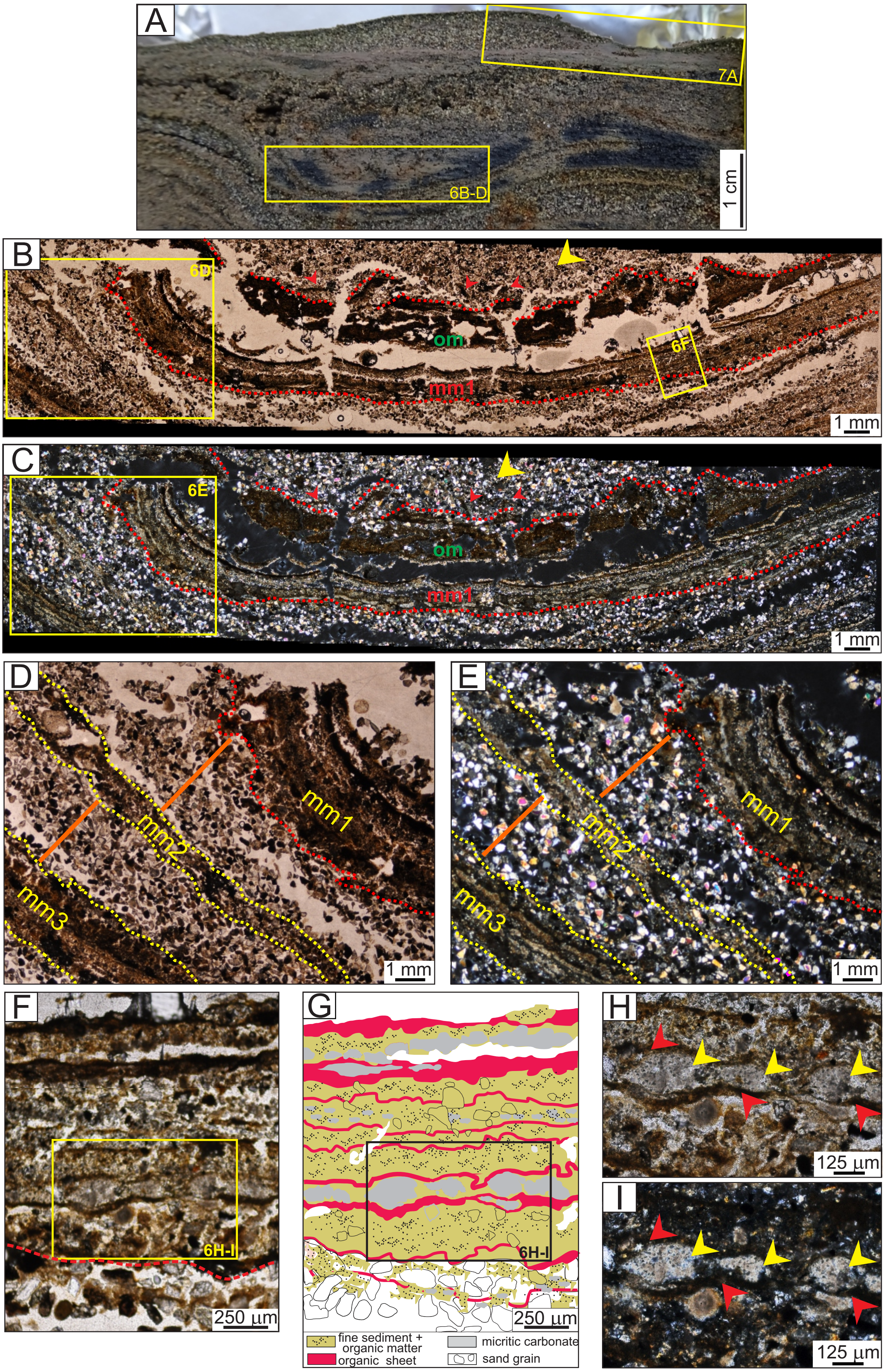
A
7A
6B-D
1 cm
B
6D
om
mm1
6F
1 mm
C
6E
om
mm1
1 mm
D
mm1
mm2
mm3
1 mm
E
mm1
mm2
mm3
1 mm
F
6H-I
250 µm
G
6H-I
250 µm
fine sediment + organic matter
organic sheet
micritic carbonate
sand grain
H
125 µm
I
125 µm

Figure 7

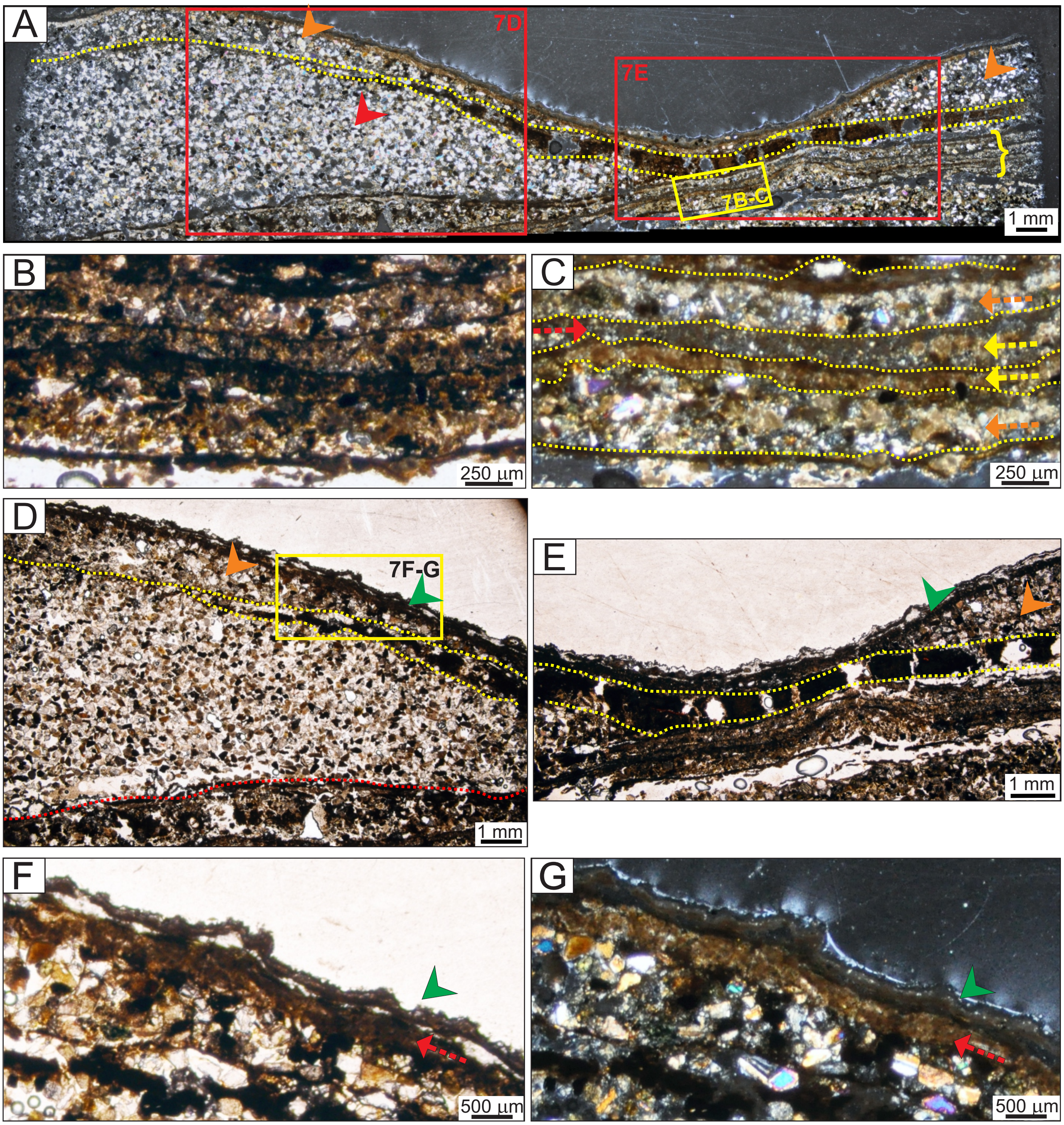

Figure 8

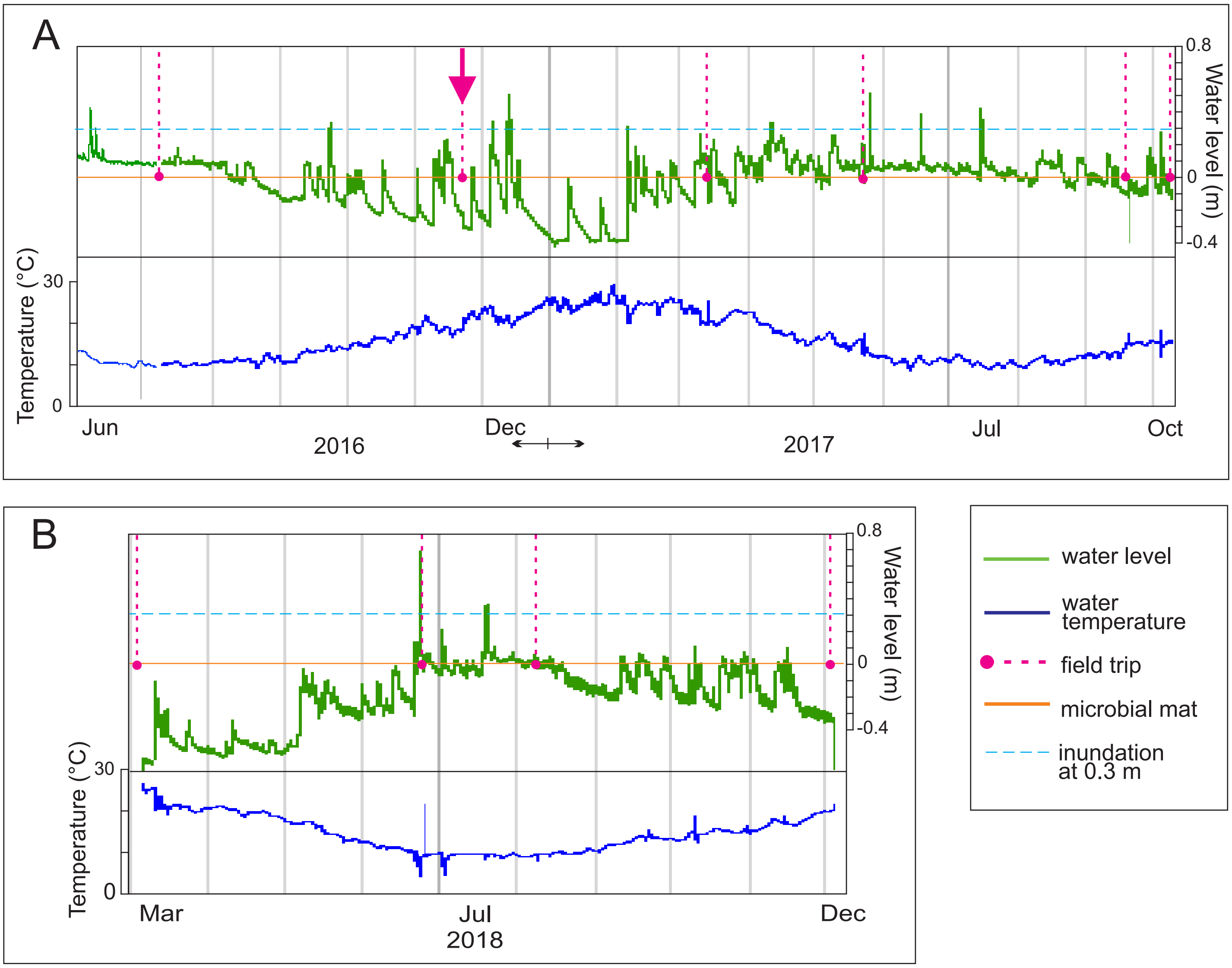
A
0.8
0
-0.4
Water level (m)
Temperature (°C)
30
0
Jun
2016
Dec
2017
Jul
Oct
B
0.8
0
-0.4
Water level (m)
Temperature (°C)
30
0
Mar
Jul
2018
Dec
water level
water temperature
field trip
microbial mat
inundation at 0.3 m

Figure 9

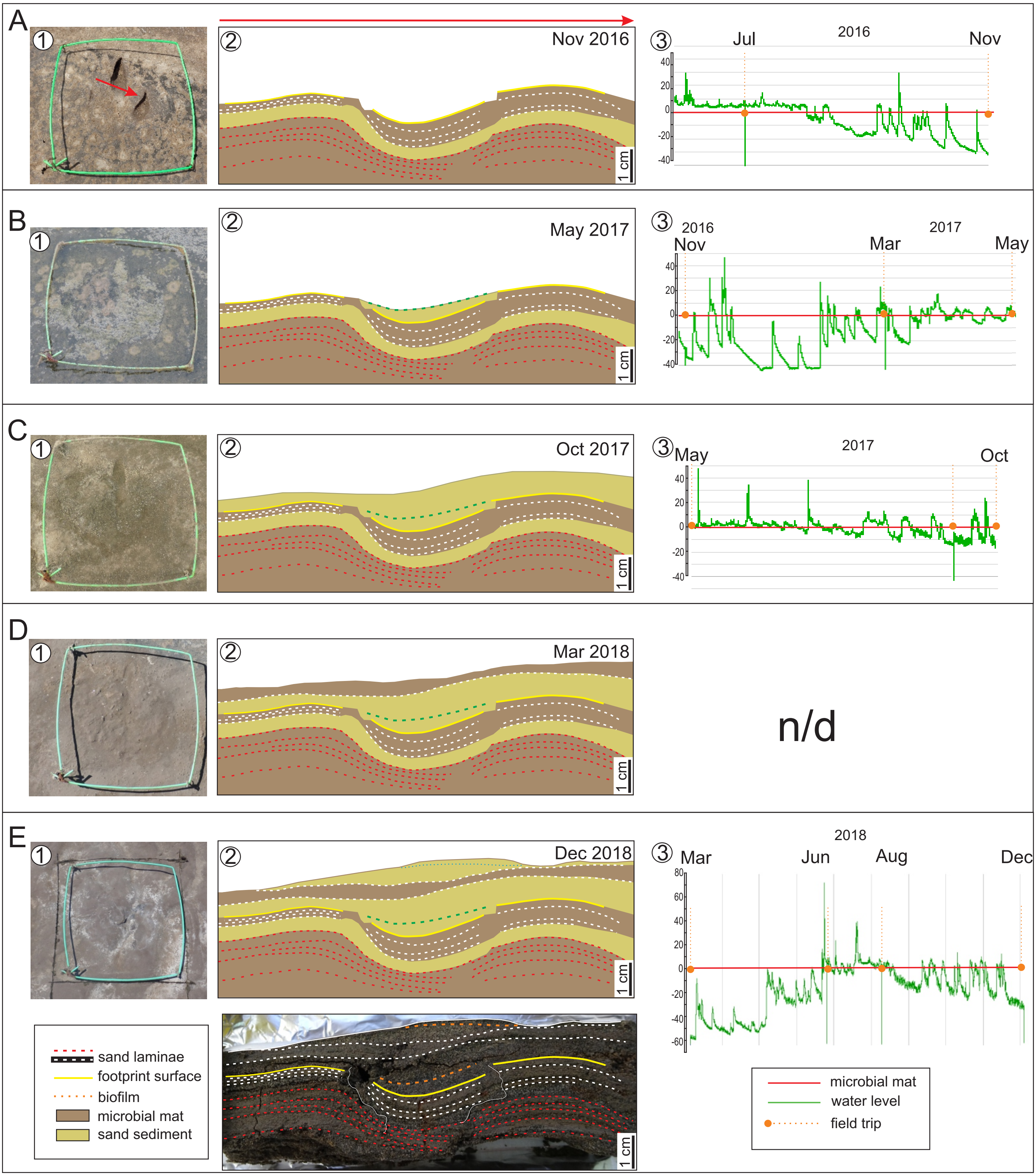
A
①
②
Nov 2016
1 cm
③
Jul
2016
Nov
40
20
0
-20
-40
B
①
②
May 2017
1 cm
③
2016
Nov
Mar
2017
May
40
20
0
-20
-40
C
①
②
Oct 2017
1 cm
③
May
2017
Oct
40
20
0
-20
-40
D
①
②
Mar 2018
1 cm
n/d
E
①
②
Dec 2018
1 cm
③
2018
Mar
Jun
Aug
Dec
80
60
40
20
0
-20
-40
-60
sand laminae
footprint surface
biofilm
microbial mat
sand sediment
1 cm
microbial mat
water level
field trip

Figure 10

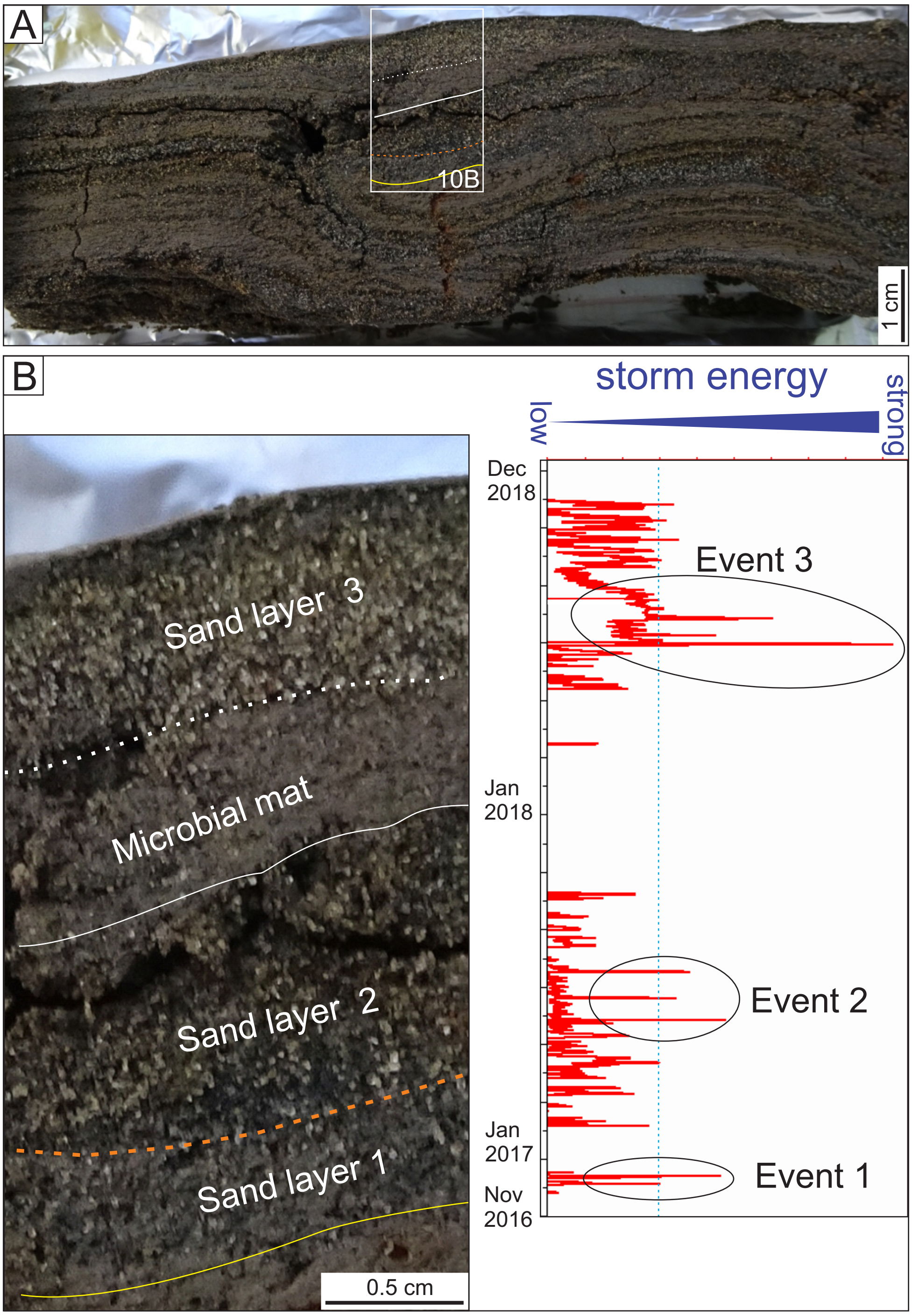
A
10B
1 cm
B
storm energy
low
strong
Sand layer 3
Microbial mat
Sand layer 2
Sand layer 1
0.5 cm
Dec 2018
Event 3
Jan 2018
Event 2
Jan 2017
Event 1
Nov 2016